Periodicals of Engineering and Natural Sciences ISSN 2303-4521
Vol. 8, No. 4, December 2020, pp.2490-2500

Studying the light current characteristics of VCSEL by changing oxide confinement aperture

Maher Faeq Mohammed[1], Nidam M. Abdul Majeed[2], Mayada J. Hamwdi[3]
[1,2,3]Kirkuk Technical College, Northern Technical University

ABSTRACT

GaAs-based VCSELs with oxide-confined (OC) are performed by using fine selective radial "oxidation of AlAs-rich (AlGaAs) layers" from outside to the device axis leaving the central part unaffected. Such oxide apertures produced inside the cavities enhance the radial confinements related to current spreading and to a field that is optical altogether. A Modern design with a single fundamental mode is proposed to reduce threshold current operation to the extent of higher output by using the two OC VCSELs. Both of the oxide apertures were added to the node position of the resonator standing wave. Then, the diameters of together apertures can be adjusted independently giving VCSEL design an extra degree of freedom that allows optimization. It found that when both apertures had a radius of 4.2 μm, the low threshold current operation at a higher extent output is achieved with a single fundamental mode.

Keywords: VCSEL, GaAs, output power, threshold current, near field, far-field

Corresponding Author:
Maher Faeq Mohammed
Kirkuk Technical College
Northern Technical University, Kirkuk, Iraq
E-mail: maher_usm@ntu.edu.iq

1. Introduction

Although a large area of VCSELs has drawn more attention in the hope of realizing convenient forms of high-power lasers, the typical VCSEL designs result in a multimode operation when the active areas are greater than 10 μm [1-3]. For some applications, the multimode operation is viewed as desirable to create a low coherence source, such as for multimode fiber signal transmission. However, a high coherence (fundamental-mode (SFM) LP_{01} operation) and a high-power source would be desirable in such optical storage [4]. Although different schemes can be used to introduce SFM LP_{01} operation laser in a large active medium, the recent VCSEL demonstrations using selective oxidation techniques have been most impressive [5]. Huffaker's and Coworkers reported the first native oxide confined VCSELs in 1994. VCSELs Modern oxide-confined (OC) which are GaAs-based [6-8], are accomplished through the careful selective radial oxidation made of AlAs-rich (AlGaAs) layers from outside to the axis of VCSEL causing no effect to their fundamental section, i.e., through establishing proper apertures of oxide. These oxide apertures created along cavities that are optical related to the VCSEL make it possible to establish radial confines of current spread and field of optics together [9]. Such limitations follow up distinct characteristics of Al_2O_3 oxides which are generated natively. i.e. through highly intensive electrical resistivity of their own in addition to refraction index which is far lower as compared with entire layers of semiconductor VCSEL [10]. Therefore, the output of the VCSELs which are oxide-confined can be substantially changed by adjusting the oxide apertures from the aspect of widths or lengths and/or places. It makes VCSEL optimizations for their different applications [11].

2. VCSEL design in numerical simulations

The 850 nm GaAs/AlGaAs top surface-emitting VCSEL was constructed with an active medium, which consists of GaAs wells with 6 nm thickness and $Al_{0.20}Ga_{0.80}As$ barriers with a thickness of 12 nm. The active medium was split between two spacers of $Al_{0.30}Ga_{0.70}As$ and two p- and n+- type DBRs. Each pair of the p- and n+- type DBRs were made by $Al_{0.20}Ga_{0.80}As$ (of high index refraction ~ 3.492) and $Al_{0.90}Ga_{0.10}As$ (of low index refraction ~ 3.062). The device with the lower section contains thirty-six pairs of n-DBRs whereas the top one contains twenty pairs with $\lambda/4$ thicknesses. A new model, in which three pairs of p in addition to n-type DBRs together are closest to the active place, where they become approximate to the spacer which is doped at

$5\times10^{+17}cm^{-3}$. While, the others are highly doped at a concentration of about $1\times10^{+19}cm^{-3}$, with 5 μm radius size which was proposed to study the effect of VCSEL oxide radius size on the design [12].

3. Simulation results and discussions for aperture oxide confinement effects

In this paper, higher-output VCSEL with 5 μm radius size without any oxide confined aperture has been designed and characterized by using ISETCAD simulation. It was found that VCSEL exhibit multimode operation.

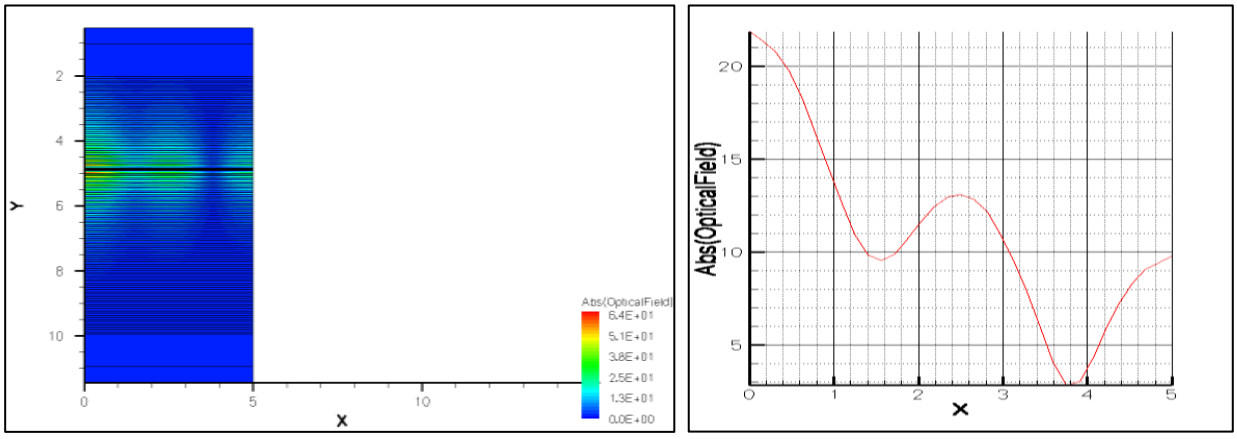

(a) (b)

Figure 1. (a) A transverse cross-sectional view and (b) Y- cut of the transverse cross-sectional view of half of the portion of MQWs 850 nm VCSEL laser format without apertures

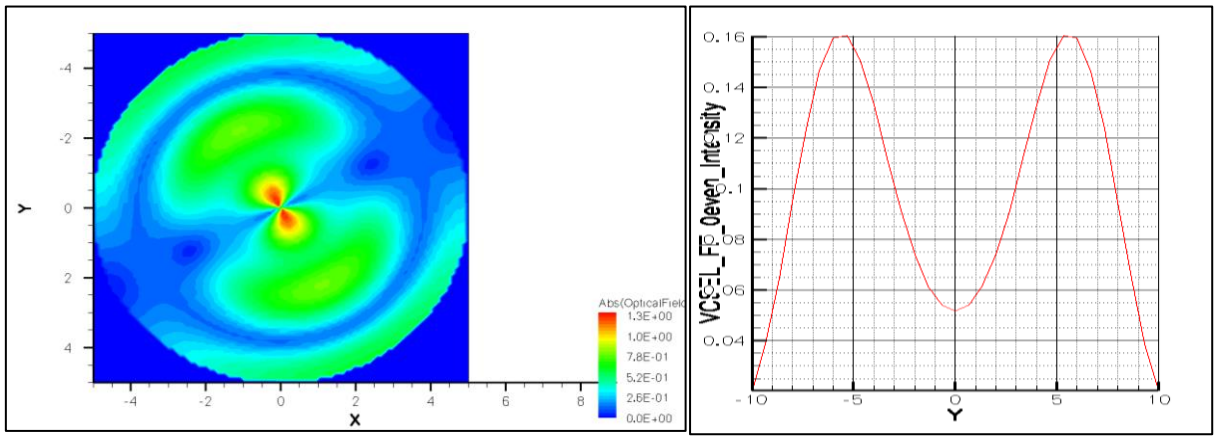

(a) (b)

Figure 2. (a) Near field pattern and (b) Y-cut of the near field pattern of MQWs 850 nm VCSEL without apertures

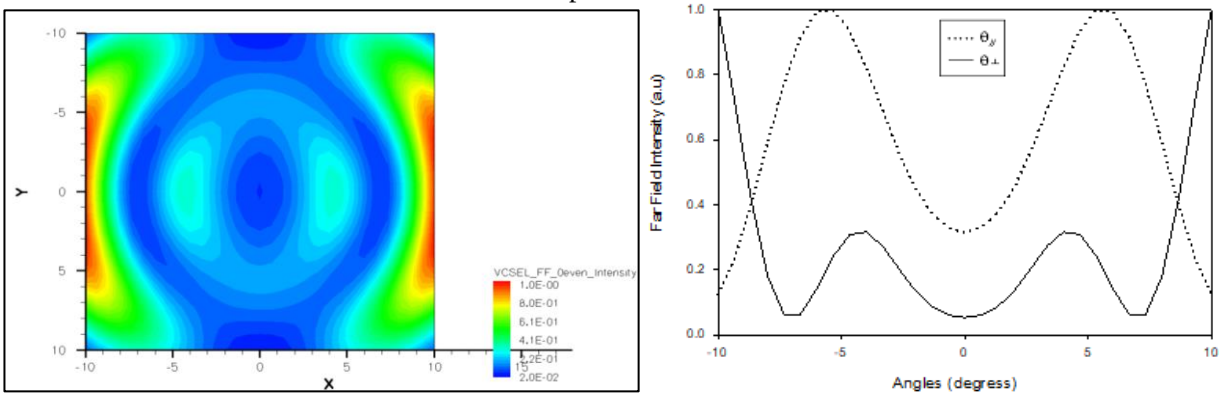

(a) (b)

Figure 3 (a) Far-field pattern and (b) $\theta_{//}$ and $\theta_{\perp}$ far-field pattern of MQWs 850 nm VCSEL format without apertures

It is mainly due to high extra non-uniform current injection into wider active areas, and barely any current enters extensive central sections of their own, while the major substantial current massing impact is noticed to be close to the edges of the active area. Due to certain radial carrier diffusion inside the active layer, the radial gain profile within active area optics is just marginally less non-uniform. Unluckily, such a profile of non-uniform gain is promising for the higher-order diagonal modes as shown in Figure 1. Figure 2 and Figure 3 show the multimode operation for higher-output VCSEL with 5 µm radius size with any aperture. However, a high coherence "single fundamental-mode (SFM) LP_{01} operation", high output power would be desirable in optical storage. Therefore, it was proposed that a VCSEL with a single oxide-confined (OC) aperture placed at the standing wave node location within the VCSEL cavity. The upper oxide aperture is separated among the layers of the p-spacer and the first p-DBR pair reducing the VCSEL lateral sizes of the principal active region. In order to give VCSEL designing an extra degree of freedom that allows optimization, the diameter, and thickness of the upper aperture were changed independently. It was observed from Figure 3 and Figure 4 that the single upper oxide aperture still showing the multimode operation. Therefore, the position of the upper single aperture was changed from last position to an aperture which is separated between the n-spacer layer and the first n-DBR pair but VCSEL was found multimode operation as shown in Figure 5, Figure 6 and Figure 7. So, it was investigated that the single oxide aperture is inadequate as radial confinement for our VCSEL design.

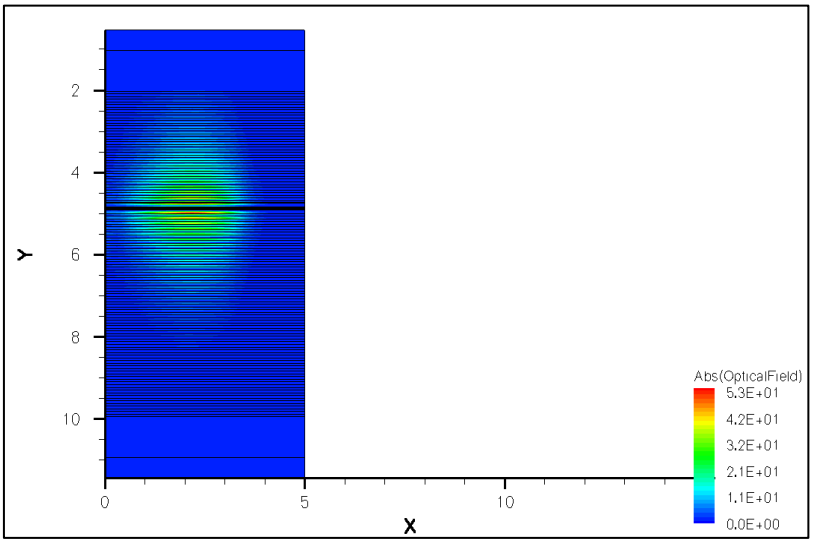

(a)

(b)

Figure 4. (a) A cross-sectional diagonal view and (b) Y-cut of cross-sectional diagonal view of the half portion of MQWs 850 nm VCSEL laser format with single upper oxide)

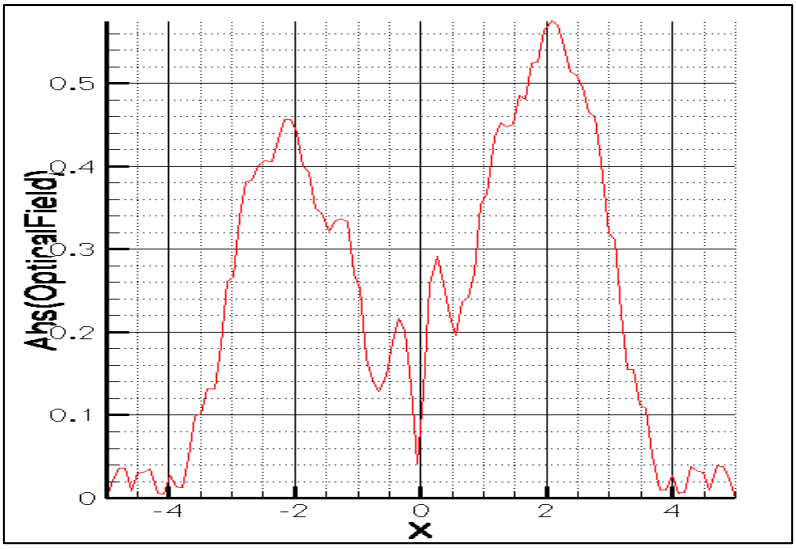

(b)

Figure 5. (a) near field area form and (b) Y-cut of the near field pattern of MQWs 850 nm VCSEL with format accompanying one upper oxide aperture

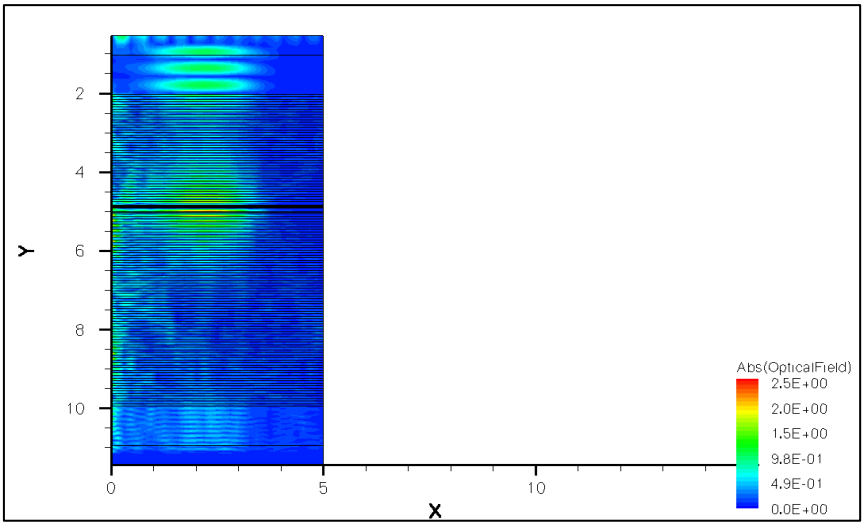

(a)

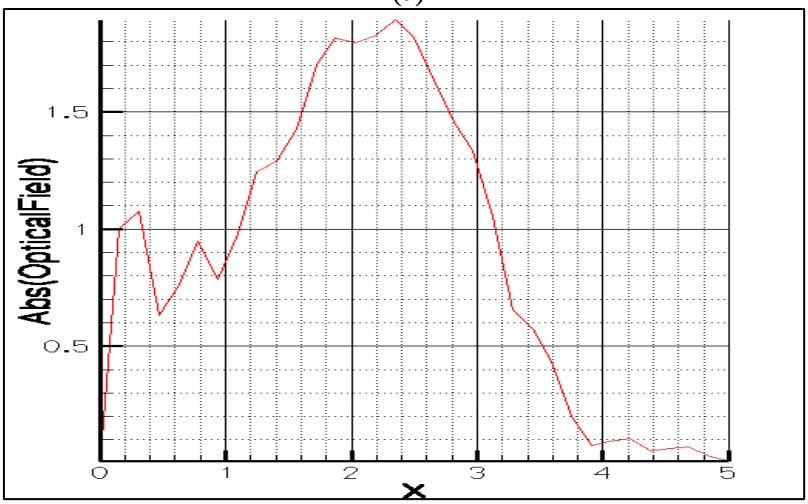

(b)

Figure 6. (a) A cross-sectional diagonal view and (b) Y-cut of cross-sectional diagonal view of the half portion of MQWs 850 nm VCSEL laser design with single lower oxide aperture.

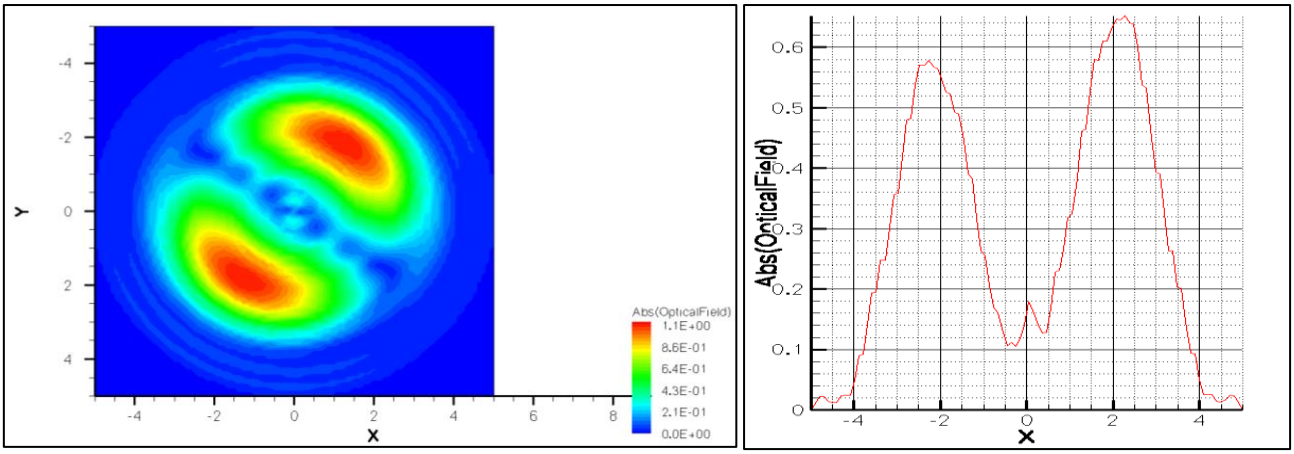

(a) (b)

Figure 7. (a) near field pattern and (b) Y-cut of the near field pattern of MQWs 850 nm VCSEL laser design with single lower oxide aperture

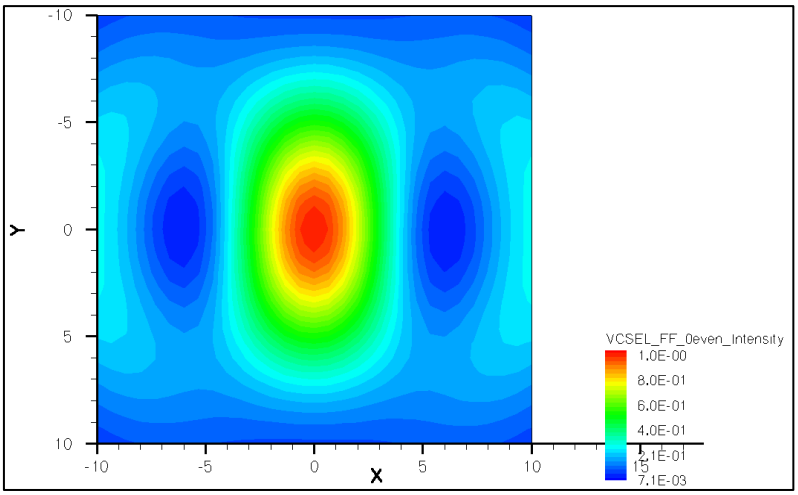

(a)

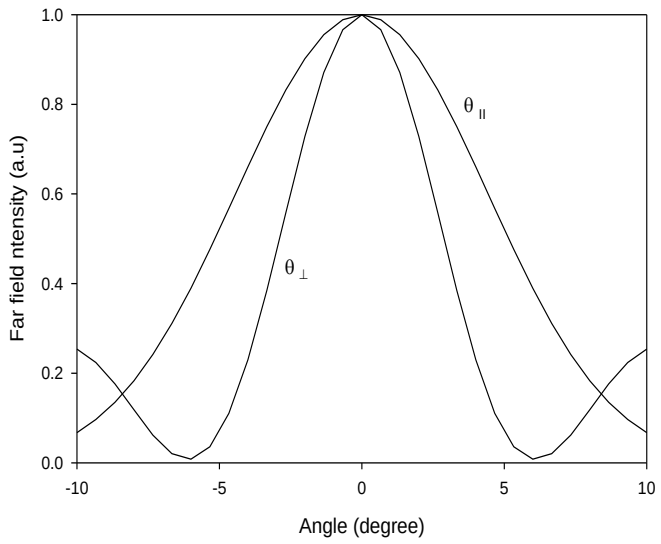

(b)

Figure 8. (a) far-field pattern and (b) $\theta_{//}$ and $\theta_{\perp}$ far-field pattern of MQWs 850 nm VCSEL design with a single oxide aperture.

The oxide-confined VCSELs performance was highly sensitive to structure specifics compared to the situation of other VCSELs

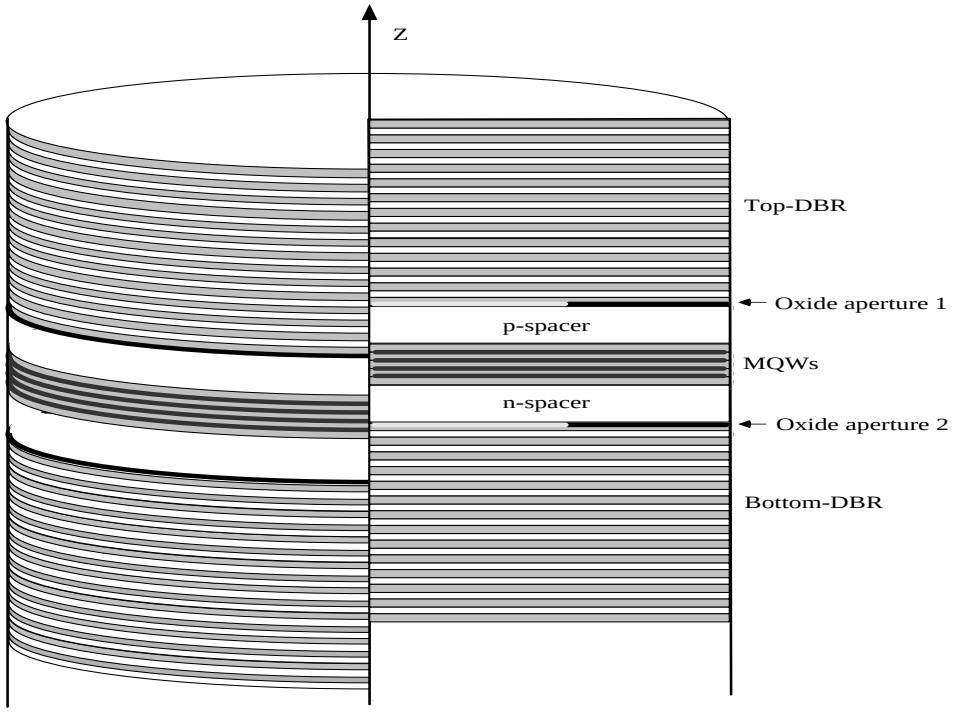

Figure 9. A cutaway view of the distinctive VCSEL model of optics, showing two oxide apertures locations

Therefore, we proposed a new VCSEL design with two oxide-confined (OC) apertures that reduce lateral dimensions of their principal active regions, oxide apertures created in optical cavities of the VCSEL allow us to establish radial confines of spreading current and an optical field together. Both of the oxide apertures with 10 nm thicknesses have to be added to the node localization of the resonator standing wave as shown in Figure 9. Figure 9 shows the inner view of the distinctive VCSEL model which is optical presenting dual oxide apertures localizations. Subsequently, the width and length of apertures altogether can be adjusted autonomously giving VCSEL design an extra degree of freedom that allows their optimization.

The diameter of apertures together can be adjusted autonomously, giving VCSEL design an extra degree of freedom which allows optimization.

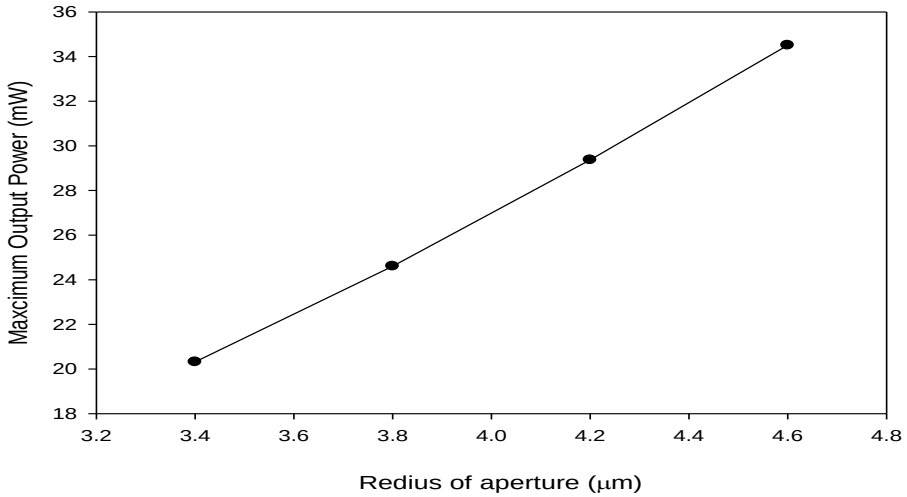

Figure 10. The variance of maximum output power with diameters of aperture

To show the distinctive characteristics of VCSELs oxide confined 850 nm with different oxide aperture dimensions. The ISETCAD simulation software is used to simulate the VCSEL device with different matching oxide aperture sizes. In terms of the dependence of their efficiencies such as output slope efficiency with differential quantum efficiency on the size of the oxide aperture, the threshold current, and the peak output power for each of these devices are calculated. The effect of the oxide aperture dimension is investigated by changing the size of the aperture from 3.4 to 4.6 μm, as displayed in Figure 10. An increase in the maximum output power was observed with an increased aperture size up to 34.85 mW for an aperture radius of 4.6 μm. It was due to the case when in wide oxide apertures, the active medium is accompanied by more lasing modes being confined within due to the increases in the number of radiative recombination inside the active region.

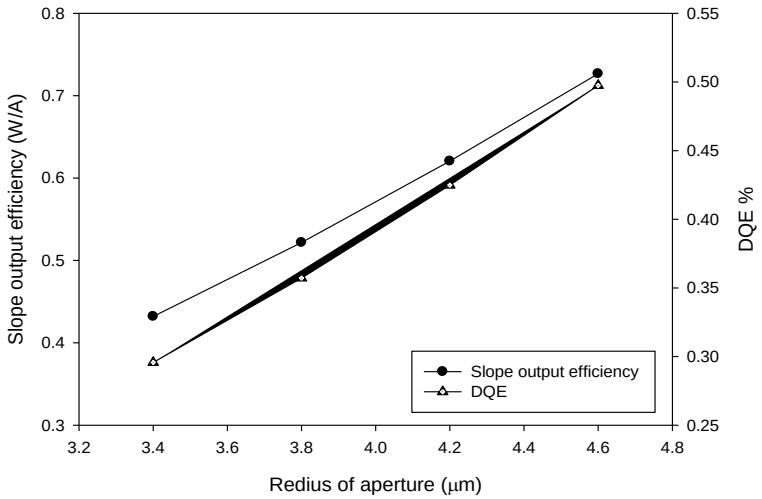

Figure 11. Variation of slope output of and efficiency of differential quantum with aperture diameter for the simulated VCSELs

The differential quantum efficiency (DQE) shows that VCSEL s efficiency in turning the electron-hole pairs injected into photons that were emitted from the device. Figure 11 shows the difference in the performance of the differential quantum efficiency and output slope efficiency with the diameter of the oxide aperture varying from 3.4 to 4.6 μm. We note that the smaller oxide aperture diameter VCSELs show decreased efficiency of slope output and efficiency of the differential quantum because of the augmented dispersion loss ensuing from oxide apertures with small wide. Figure 12 indicates the threshold current variation along the aperture diameter for the virtual VCSELs. Figure 12 shows that the lowest threshold current was obtained when the diameter of the apertures was 4.2 μm.

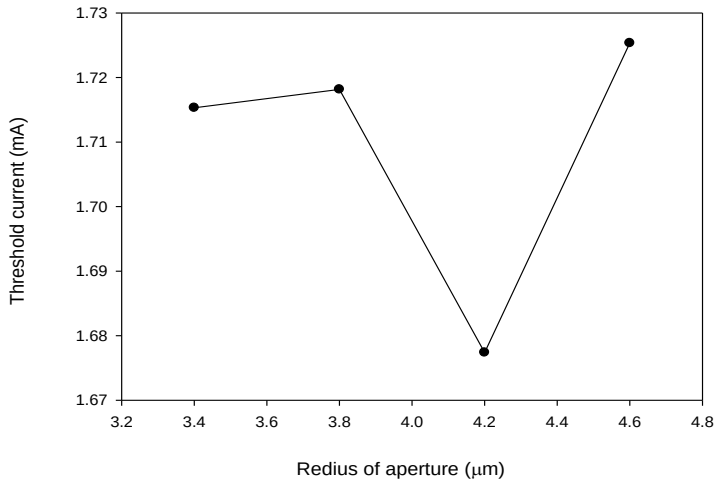

Figure 12. The threshold current variation with aperture diameter for the virtual VCSELs

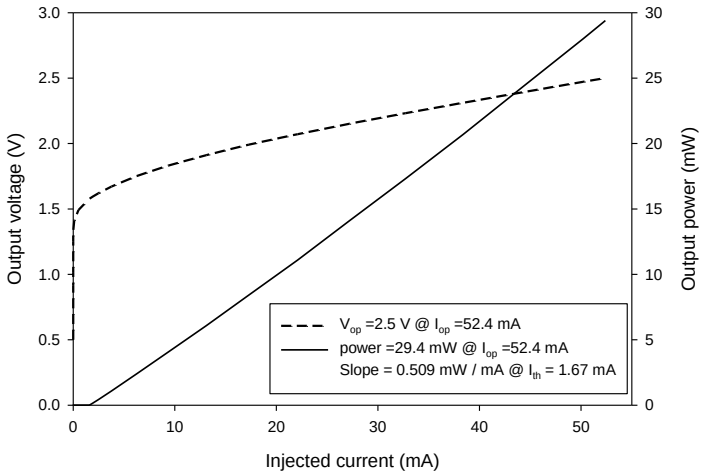

Figure 13. Power output and voltage as a function of injecting current

To get a single fundamental mode with higher power output and lower threshold current, a new design with two OC VCSEL is proposed. It was found that for both apertures with 4.2 μm diameters, one basic mode with low threshold current action at the higher output was achieved with two OC VCSELs. Adding the two apertures lead to relatively small active regions only inside the active region, which makes single fundamental mode (SFM) output VCSEL available in addition to reducing the threshold current from1.77 to 1.67 mA. Figure 7.30 shows the power output and voltage as an injection current function. The power output of 29.4 mW, the threshold current of 1.67 mA, and the threshold voltage are 1.31 V while the external voltage of 2.5 V was obtained from structures that are purely cylindrical with a radius of 5 μm with two oxide confinements. The efficiency of slope output and differential quantum efficiency (DQE) is the basic parameters of the performance of the VCSEL. The slope efficiency of 0.621 and DQE is found to be 0.683 at an emission wavelength of 847.70 nm just as shown in Figure 14.

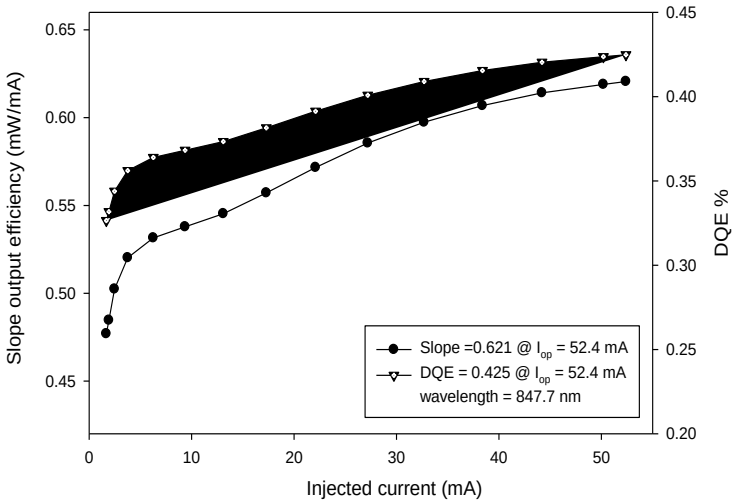

Figure 14. Voltage and power of the output as an injection current function for a VCSEL design with two oxide apertures

Figure 15 shows the effect of two oxide apertures on the distribution of density of carriers (including electrons and holes) within the MQWs active region. The n-side on the right side of the diagram and the p-side of the GaAs VCSEL on the left side. The distance within the active medium along the direction of the crystal growth inside is the horizontal axis. It is possibly noticed that two oxide apertures cause an increase in the redial confinement inside the VCSEL. Therefore, a rapid increase for both electrons and holes carriers' density was observed.

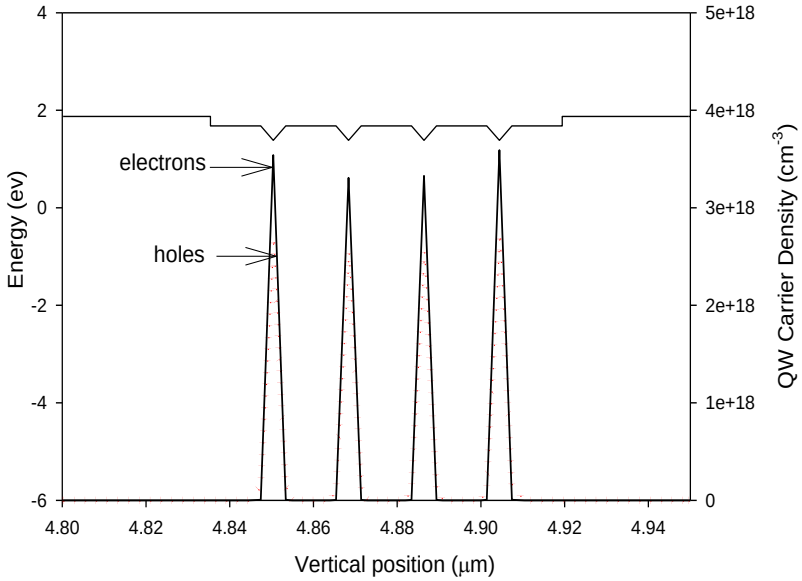

Figure 15. Density distribution of electron and holes carrier inside the MQWs active region for a VCSEL design with two oxide apertures

In the active region, more carrier density can be confined, often contributing to increase the gain of material which is optical inside the good layers quantum as viewed in Figure 16. Figure 16 shows optical material gain increased within the quantum well layers by adding two oxide apertures to the structure of GaAs VCSEL. As a resulting rise in the prospect of stirred release in one cavity pass, it increases the gain within the active region of MQWs. It is observed that for both apertures with 4.2 μm diameters, the single fundamental mode was achieved, which makes single fundamental mode (SFM) output VCSEL available as shown in Figure 17. Figure 17 shows the transverse cross-sectional view of the half portion of VCSEL with two oxide apertures which is showing the SFM output operation. The investigations of near characteristics of the designed VCSEL with two oxide confined apertures have been performed as shown in Figure 7.35. By adding the oxide confined aperture, the near field pattern and y-cut show the transverse mode, which is a mode of a single order.

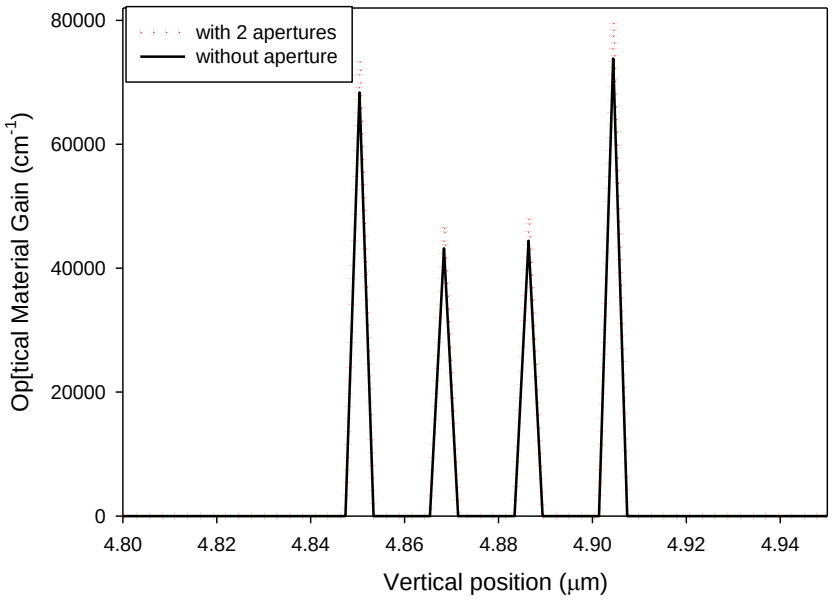

Figure 16. Optical material gain inside the MQWs active region for a VCSEL design with two oxide apertures

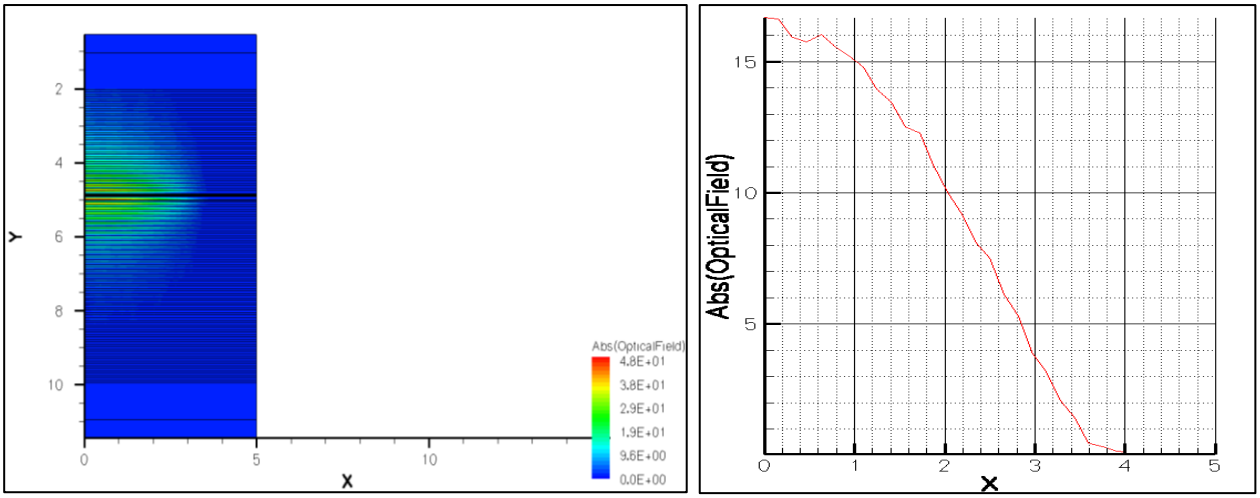

(a) (b)

Figure 17. (a) A transverse cross-sectional view and (b) Y-cut of the transverse cross-sectional view of the half portion of MQWs 850 nm VCSEL laser design with two oxide apertures

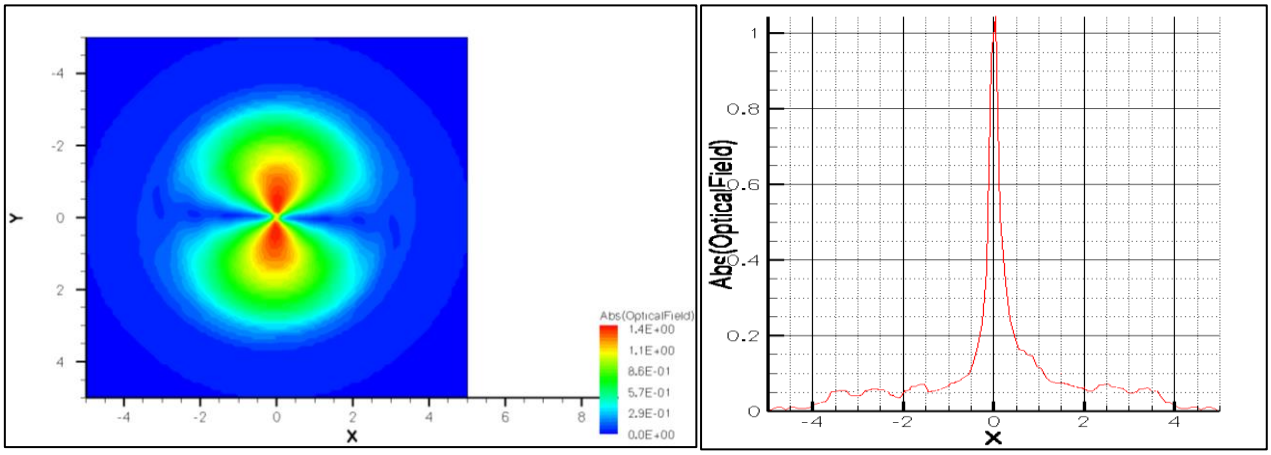

(a) (b)

Figure 18.The near field pattern and (b) Y-cut of the near field pattern of MQWs 850 nm VCSEL laser design with two oxide apertures

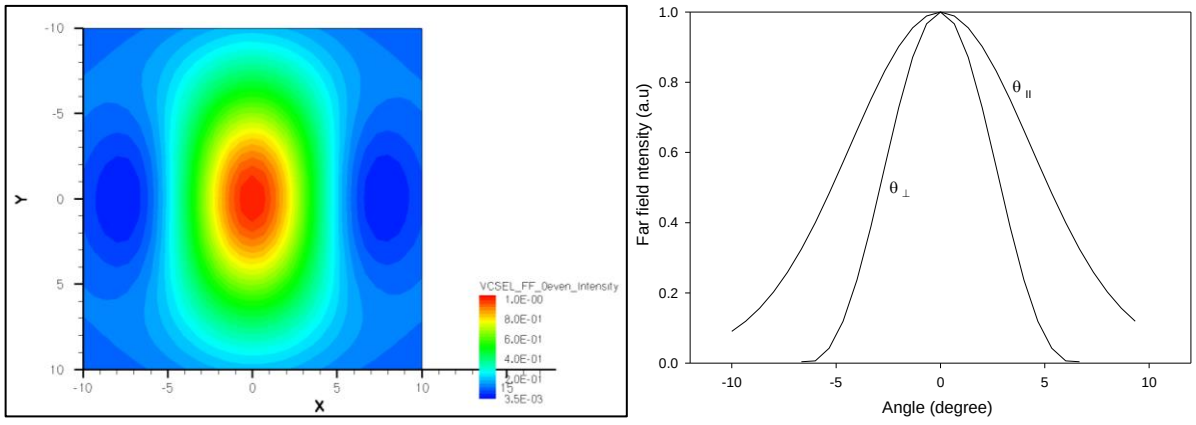

(a) (b)

Figure 19. (a) far-field pattern and (b) $\theta_{//}$ and $\theta_{\perp}$ far-field pattern of MQWs 850 nm VCSEL design with two oxide apertures

The investigations of far-field pattern characteristics of the designed VCSEL with two oxide confined apertures have also been performed as shown in Figure 19. The radiative form emanating out of our proposed design is shown in Figure 19 (a) and Figure 19 (b) respectively, which $\theta_{//}$ and $\theta_{\perp}$ signify respectively the full angle of half power in the directions parallel and perpendicular to the plane of the junction. The values of 6º and 12º are respectively attained for the FWHM $\theta_{\perp}$ and FWHM $\theta_{//}$. It was noticed from the proximate field and distant field that the diagonal mode is a mode of one order related to two oxide apertures.

4. Conclusion

Increasing the area of VCSELs designs lead to a multimode operation. For some applications, the multimode mode operation is viewed as desirable to create a low coherence source, such as for multimode fiber signal transmission However, a high coherence (fundamental-mode (SFM) LP_{01} operation), the high power source is desirable such in optical storage. In particular, it is difficult to achieve a stable single fundamental mode operation in those VCSELs particularly with higher output and large size operating devices. The effect of VCSELs oxide radius size on the output power, threshold current, slope, and differentials quantum efficiency is observed. To get one basic mode with low threshold current operation at higher output, a novel design of VCSEL is proposed with twofold OC apertures. Both of the oxide apertures should be added to the node position of the resonator standing wave. Then, the diameters of both apertures can be adjusted independently, giving VCSEL design an extra degree of freedom that allows their optimization. It noticed when both apertures have a radius of 4.2 μm, one basic mode was achieved with low threshold current operation at the higher output with two OC VCSEL.

References

[1] J. Cheng and N. K. Dutta, *Vertical-cavity surface-emitting lasers: technology and applications* vol. 10: CRC Press, 2000.

[2] A. M. Sharizal, P. O. Leisher, K. D. Choquette, P. Choudhury, S. M. Mitani, Y. M. Razman, *et al.*, "Effect of oxide aperture on the performance of 850 nm vertical-cavity surface-emitting lasers," *Optik*, vol. 120, pp. 121-126, 2009.

[3] M. Streiff, "Opto-electro-thermal VCSEL device simulation," ETH Zurich, 2004.

[4] F. Mederer, C. Jung, R. Jager, M. Kicherer, R. Michalzik, P. Schnitzer, *et al.*, "12.5 Gbit/s data rate fiber transmission using single-mode selectively oxidized GaAs VCSELs at/spl lambda/= 850 nm," in *1999 IEEE LEOS Annual Meeting Conference Proceedings. LEOS'99. 12th Annual Meeting. IEEE Lasers and Electro-Optics Society 1999 Annual Meeting (Cat. No. 99CH37009)*, 1999, pp. 697-698.

[5] G. Yang, M. MacDougal, and P. Dapkus, "Ultralow threshold current vertical-cavity surface-emitting lasers obtained with selective oxidation," *Electronics Letters*, vol. 31, pp. 886-888, 1995.

[6] S. Mitani, P. Choudhury, and M. Alias, "On the characterization of a new type of oxide-confined 850 nm GaAs-based vertical-cavity surface-emitting laser," *Optik*, vol. 119, pp. 373-378, 2008.

[7] H. Martinsson, J. Vukusic, and A. Larsson, "Single-mode power dependence on surface relief size for mode-stabilized oxide-confined vertical-cavity surface-emitting lasers," *IEEE Photonics Technology Letters*, vol. 12, pp. 1129-1131, 2000.

[8] K. L. Lear and A. N. Al-Omari, "Progress and issues for high-speed vertical cavity surface emitting lasers," in *Vertical-Cavity Surface-Emitting Lasers XI*, 2007, p. 64840J.

[9] I. A. Aljazaery, H. Alhasan, F. N. Al Hachami, and H. Alrikabi, "Simulation Study to Calculate the Vibration Energy of Two Molecules of Hydrogen Chloride and Carbon Oxide," *Journal of Green Engineering*, vol. 10, pp. 5989-6010, 2020.

[10] S. Bader, P. Gerlach, and R. Michalzik, "Optically controlled current confinement in vertical-cavity surface-emitting lasers," *IEEE Photonics Technology Letters*, vol. 28, pp. 1309-1312, 2016.

[11] D. Deppe, J. Leshin, L. Eifert, F. Tucker, and T. Hillyer, "Transverse mode confinement in lithographic VCSELs," *Electronics Letters*, vol. 53, pp. 1598-1600, 2017.

[12] T. Sarmiento, L. Zhao, P. Moser, T. Li, Y. Huo, and J. S. Harris, "Continuous-Wave Operation of GaAs-Based 1.5-$\mu $ m GaInNAsSb VCSELs," *IEEE Photonics Technology Letters*, vol. 31, pp. 1607-1610, 2019.